SEGMENTATION BASED SATELLITE IMAGE FUSION USING FAST GUIDED FILTER

A PROJECT REPORT

Submitted by

VARSHALAKSHMI S

Register No: 15MAE012

in partial fulfillment for the requirement of award of the degree

of

MASTER OF ENGINEERING

in

APPLIED ELECTRONICS

Department of Electronics and Communication Engineering

KUMARAGURU COLLEGE OF TECHNOLOGY

(An autonomous institution affiliated to Anna University, Chennai)

COIMBATORE-641049

ANNA UNIVERSITY: CHENNAI 600 025

APRIL 2017

BONAFIDE CERTIFICATE

Certified that this project report titled **"SEGMENTATION BASED SATELLITE IMAGE FUSION USING FAST GUIDED FILTER"** is the bonafide work of **VARSHALAKSHMI.S [Reg. No. 15MAE012]** who carried out the research under my supervision. Certified further, that to the best of my knowledge the work reported herein does not form part of any other project or dissertation on the basis of which a degree or award was conferred on an earlier occasion on this or any other candidate.

SIGNATURE

Ms. S.NAGARATHINAM

PROJECT SUPERVISOR

Department of ECE

Kumaraguru College of Technology

Coimbatore-641 049

SIGNATURE

Prof. K.RAMPRAKASH

HEAD OF THE DEPARTMENT

(PG Programme)

Department of ECE

Kumaraguru College of Technology

Coimbatore-641 049

The Candidate with **Register No. 15MAE012** was examined by us in the project viva-voice examination held on ……..

INTERNAL EXAMINER **EXTERNAL EXAMINER**

ACKNOWLEDGEMENT

First, I would like to express my praise and gratitude to the Lord, who has showered his grace and blessings enabling me to complete this project in an excellent manner.

I express my sincere thanks to the management of Kumaraguru College of Technology and Joint Correspondent **Shri Shankar Vanavarayar** for his kind support and for providing necessary facilities to carry out the work.

I would like to express my sincere thanks to our beloved Principal **Dr.R.S.Kumar Ph.D.,** Kumaraguru College of Technology, who encouraged us with his valuable thoughts.

I would like to thank **Prof. K.Ramprakash M.E.,** Head of the Department, (PG Programme), Electronics and Communication Engineering, for his continuous encouragement and motivation throughout the course of this project work.

In particular, I wish to thank with everlasting gratitude to the Project Coordinator and my project guide **Ms.S.Nagarathinam M.E., (Ph.D).,** Assistant Professor-III, Department of Electronics and Communication Engineering, for her expert counselling and guidance to make this project to a great deal of success and I wish to convey my deep sense of gratitude to all teaching and non-teaching staff of ECE Department for their help and cooperation.

Finally, I thank my parents and my family members for giving me the moral support and abundant blessings in all of my activities and my dear friends who helped me to endure my difficult times with their unfailing support and warm wishes.

ABSTRACT

In remote sensing, satellites provide panchromatic (PAN) image of high spatial resolution and multispectral (MS) image of high spectral resolution. Several applications require both spatial and spectral resolution to be high in a single image. This can be made possible by using image fusion techniques which merges PAN and MS image resulting in high quality image. Guided image filter is one of the recent edge preserving filters used in image processing which preserves the edges and at the same time preserves the edge information. A novel image fusion method using fast guided image filtering is proposed which tends to provide the complexity of $O(N/s^2)$ for an image with N pixels than that of guided image filter with the complexity of $O(N)$. This tends to give the advantage of removing the artifacts in the image with reduced computational complexity. The source images undergo two-scale decomposition into a base and a detail layer holding large and small details of the image respectively. Image segmentation is one of the important tools for image enhancement which divides the image into multiple segments thereby converting the image into something that is more meaningful helping in further processing and analysis. Optimization based segmentation was applied to the source images to perform fusion in an effective way. The performance of various segmentation techniques was analyzed and their results have been compared by evaluating various metrics applied to the resultant fused image. In addition, Elapsed time is computed to show the significance of fast guided filter. The proposed method tends to provide the better quality fused image than the other methods. The source images that are used are from Ikonos and QuickBird sensor.

TABLE OF CONTENTS

CHAPTER NO	TITLE	PAGE NO
	ABSTRACT	**iv**
	LIST OF FIGURES	**vii**
	LIST OF TABLES	**viii**
	LIST OF ABBREVIATIONS	**ix**
1	**INTRODUCTION**	**1**
	1.1 Overview	1
	1.2 Satellite Remote Sensing	1
	1.3 Types of Satellite Images	3
	1.4 Types of Resolution	4
	1.5 Image Fusion	5
	1.6 Image Segmentation	6
	1.7 Image Segmentation Techniques	6
	1.7.1 Thresholding	6
	1.7.2 Clustering	7
	1.8 Guided Image Filtering (GIF)	7
	1.9 Fast Guided Image Filtering (FGIF)	8
2	**LITERATURE SURVEY**	**10**
3	**METHODOLOGY**	**16**
	3.1 Introduction	16
	3.2 K-means Clustering	16
	3.3 Fuzzy C Means (FCM) Clustering	17
	3.4 Modified Fuzzy C Means (MFCM) Clustering	18
	3.5 Particle Swarm Optimisation (PSO) Segmentation	19
	3.6 Modified Particle Swarm Optimisation (MPSO)	

Segmentation 20
3.7 Guided Image Filtering (GIF) Computation 21
3.8 Algorithm for GIF and FGIF 23
3.9 Block Diagram 24
3.9.1 Two-scale Image Decomposition 25
3.9.2 Saliency Map Construction 26
3.9.3 Weight Map Construction 26
3.9.3 Two-scale Image Reconstruction 27
4 SIMULATION RESULTS 28
4.1 Results 28
4.1.1 Input Images of Ikonos Sensor 28
4.1.2 Input Images of QuickBird Sensor 29
4.2 Quality Metrics for Performance Evaluation 30
4.3 Comparison of various Segmentation Algorithms 32
4.4 Comparison for Guided and Fast Guided Filter 35
5 CONCLUSION AND FUTURE WORK 38
REFERENCES 39
LIST OF PUBLICATIONS 42

LIST OF FIGURES

FIGURE NO.	CAPTION	PAGE NO.
1.1	Spectrum of Objects	2
1.2	Advantage of image fusion	5
1.3	Guided Image Filtering	6
3.1	Window Choice	22
3.2	Block Diagram	25
4.1	Panchromatic and Multispectral Images of Ikonos Sensor	29
4.2	Panchromatic and Multispectral Images of QuickBird Sensor	30
4.3	Fusion results of proposed method without and with different segmentation techniques for the input images in fig. 4.1.	33
4.4	Fusion results of proposed method without and with different segmentation techniques for the input images in fig. 4.2.	34
4.5	Bar Graph representation of the elapsed time taken by different segmentation algorithms using guided and fast guided filter applied on Ikonos images	36
4.6	Bar Graph representation of the elapsed time taken by different segmentation algorithms using guided and fast guided filter applied on QuickBird images	36
4.7	Elapsed time for different sampling ratios (s= 1 to 10) based on MPSO segmentation applied on Ikonos images	37
4.8	Elapsed time for different sampling ratios (s= 1 to 10) based on MPSO segmentation applied on QuickBird images.	37

LIST OF TABLES

TABLE NO.	CAPTION	PAGE NO.
4.1	Spectral Resolution of Ikonos Sensor	28
4.2	Spectral Resolution of QuickBird Sensor	29
4.3	Quality metrics corresponding to six fusion results in fig. 4.3.	33
4.4	Quality metrics corresponding to six fusion results in fig. 4.4.	34

LIST OF ABBREVIATIONS

RADAR	Radio Detection and Ranging
PAN	Panchromatic Image
MS	Multispectral Image
RGB	Red Green Blue
HDT	Histogram Dependent Technique
EMT	Edge Maximization Technique
GIF	Guided Image Filtering
FGIF	Fast Guided Image Filtering
MRF	Markov Random Field
WLS	Weighted Least Square
NSCT	Non-Sampled Contourlet Transform
TV	Total Variation
WGIF	Weighted Guided Image Filter
FCM	Fuzzy C Means
MFCM	Modified Fuzzy C Means
PSO	Particle Swarm Optimization
MPSO	Modified Particle Swarm Optimization
SI	Swarm Intelligence
MSE	Mean Square Error

PSNR	Peak Signal to Noise Ratio
SSIM	Structural Similarity Index Measure
NK	Normalized Cross Correlation
NAE	Normalized Absolute Error
FPGA	Field Programmable Gate Array

CHAPTER 1

INTRODUCTION

1.1 OVERVIEW

Remote sensing is the process of acquiring data or information about objects and substances not in direct contact with the sensor, by gathering its inputs using electromagnetic radiation or acoustical waves that emanate from the targets of interest. Remote sensing makes it possible to collect data on dangerous or inaccessible areas. Remote sensing also replaces costly and slow data collection on the ground, ensuring in the process that areas or objects are not disturbed. The sun is a source of energy or radiation, which provides a very convenient source of energy for remote sensing. The sun's energy is either reflected, as it is for visible wavelengths, or absorbed and then reemitted, as it is for thermal infrared wavelengths. There are two main types of remote sensing: Passive remote sensing and Active remote sensing.

Passive remote sensing - Remote sensing systems which measure energy that is naturally available are called passive sensors. The sensor records energy that is reflected such as visible wavelengths from the sun or emitted (thermal infrared) from the source. Examples of passive remote sensors include film photography, infrared, and radiometers.

Active remote sensing - Active sensors emits energy in order to scan objects or areas. It then detects and measures the radiation that is reflected or backscattered from the target. RADAR is an example of active remote sensing where the time delay between emission and return is measured, establishing the location, height, speeds and direction of an object.

1.2 SATELLITE REMOTE SENSING

Remote sensing images are acquired by earth observation satellites. These remote sensing satellites are equipped with sensors looking down to the earth. Orbital platforms collect and transmit data from different parts of the electromagnetic spectrum, which in conjunction with larger scale aerial or ground-based sensing and analysis provides researchers with enough information to monitor trends. Satellite

sensors record the intensity of electromagnetic radiation (sunlight) reflected from the earth at different wavelengths. Energy that is not reflected by an object is absorbed. Each object has its own unique 'spectrum' as shown in fig 1.1.

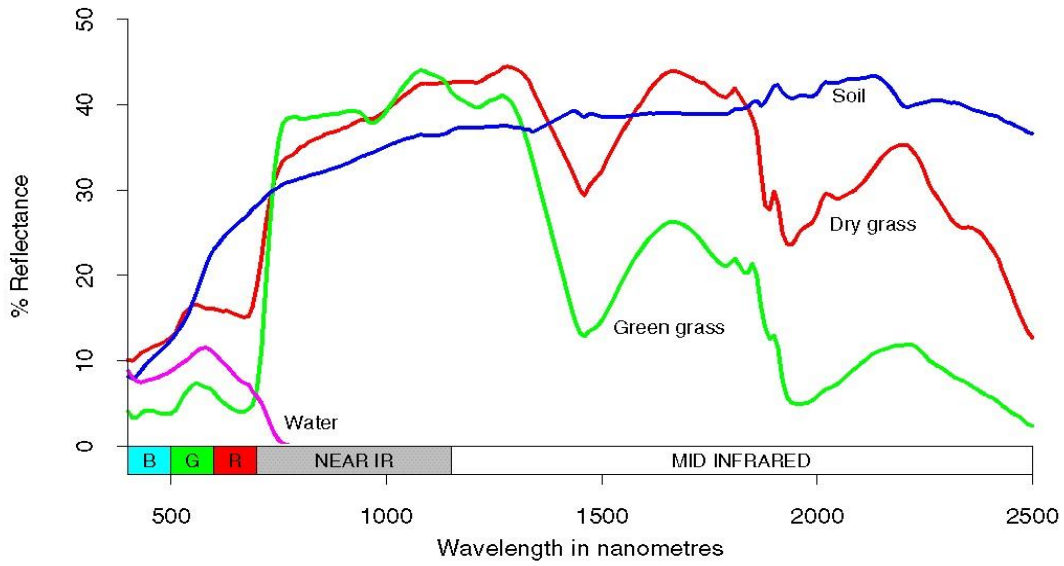

Fig. 1.1. Spectrum of Objects

Remote sensing relies on the fact that particular features of the landscape such as bush, crop, salt-affected land and water reflect light differently in different wavelengths. Grass looks green, for example, because it reflects green light and absorbs other visible wavelengths. This can be seen as a peak in the green band in the reflectance spectrum for green grass above. The spectrum also shows that grass reflects even more strongly in the infrared part of the spectrum. This can't be detected by the human eye but it can be detected by an infrared sensor. Instruments mounted on satellites detect and record the energy that has been reflected. The detectors are sensitive to particular ranges of wavelengths, called 'bands'. The satellite systems are characterised by the bands at which they measure the reflected energy.

The Landsat TM satellite, which provides the data used in this project, has bands at the blue, green and red wavelengths in the visible part of the spectrum and at three bands in the near and mid infrared part of the spectrum and one band in the thermal infrared part of the spectrum. The satellite detectors measure the intensity of the reflected energy and record it.

1.3 TYPES OF SATELLITE IMAGES

- Panchromatic image
- Multispectral image
- Hyperspectral image

Panchromatic image

A panchromatic image consists of only one band. Thus, a panchromatic image may be similarly interpreted as a black-and-white aerial photograph of the area. Panchromatic image is usually displayed as a grayscale image, i.e. the displayed brightness of a particular pixel is proportional to the pixel digital number which is related to the intensity of solar radiation reflected by the targets in the pixel and detected by the detector. The spectral information or "colour" of the targets is lost. Ikonos Pan, QuickBird Pan, SPOT Pan, LANDSAT ETM+ Pan are an example of panchromatic sensor.

Multispectral image

A multispectral image is one that captures image data at specific frequencies across the electromagnetic spectrum. A multispectral image consists of several bands of data. For visual display, each band of the image may be displayed one band at a time as a grayscale image, or in combination of three bands at a time as a colour composite image. It is a multilayer image which contains both the brightness and spectral information of the targets being observed. Multispectral data sets are usually composed of about 5 to 10 bands of relatively large bandwidths (70-400 nm). Landsat TM, MSS, Spot HRV-XS, Ikonos MS, QuickBird MS is an example of multispectral imaging.

Hyperspectral Image

It acquires images in about a hundred or more contiguous spectral bands. The precise spectral information contained in a hyperspectral image enables better characterisation and identification of targets. Hyperspectral images are of high spectral resolution compared to panchromatic and multispectral images. Hyperspectral data sets are generally composed of about 100 to 200 spectral bands of relatively narrow bandwidths (5-10 nm). The Hyperion is an example of a hyperspectral sensor.

Colour Composite Images

In displaying a colour composite image, three primary colours RGB (red, green and blue) are used. When these three colours are combined in various proportions, they produce different colours in the visible spectrum. Associating each spectral band (not necessarily a visible band) to a separate primary colour produces a colour composite image.

1.4 TYPES OF RESOLUTION

In remote sensing the term resolution is used to represent the resolving power, which includes not only the capability to identify the presence of two objects, but also their properties. In qualitative terms resolution is the amount of details that can be observed in an image. Four types of resolutions are defined for the remote sensing systems.

Spatial Resolution

Spatial resolution is a measure of the area or size of the smallest dimension on the Earth's surface over which an independent measurement can be made by the sensor. It is expressed by the size of the pixel on the ground in meters.

Radiometric Resolution

Radiometric Resolution refers to the smallest change in intensity level that can be detected by the sensing system. The intrinsic radiometric resolution of a sensing system depends on the signal to noise ratio of the detector.

Spectral resolution

It is used to describe the ability of a sensor to distinguish between wavelength intervals in the electromagnetic spectrum (bands). The finer the spectral resolution, the narrower the wavelength ranges for a particular channel or band.

Temporal resolution

Temporal resolution is a measure of how often data are obtained for the same area. The temporal resolution specifies the revisiting frequency of a satellite sensor for a specific location.

1.5 IMAGE FUSION

In remote sensing applications, the increasing availability of space borne sensors gives a motivation for different image fusion algorithms. Image fusion is an effective technique to integrate spatial and spectral information of the PAN and MS images. Through remote sensing image fusion technique, we cannot only overcome the limitation of information obtained from individual sensor but also achieve a better observation. Image fusion has been used in many application areas. In remote sensing multi-sensor fusion is used to achieve high spatial and spectral resolutions by combining images from two sensors, one of which has high spatial resolution and the other one high spectral resolution.

Several situations in image processing require high spatial and high spectral resolution in a single image. Most of the available equipment is not capable of providing such data convincingly. Image fusion techniques allow the integration of different information sources. The fused image can have complementary spatial and spectral resolution characteristics. However, the standard image fusion techniques can distort the spectral information of the multispectral data while merging. Advantage of image fusion is given in fig. 1.2. Image fusion techniques can improve the quality and increase the application of these data. At the receiver station, the panchromatic image is merged with the multispectral data to convey more information. The images used in image fusion should already be registered.

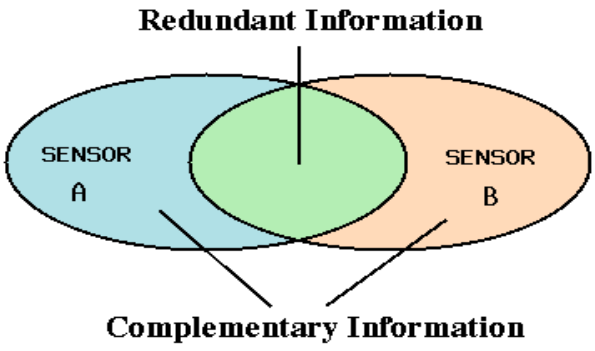

Fig. 1.2. Advantage of image fusion

Many methods exist to perform image fusion. The very basic one is the high pass filtering technique. Later techniques are based on Discrete Wavelet Transform, uniform rational filter bank, and Laplacian pyramid.

A multispectral image can be bundled with a higher-resolution, panchromatic image. This allows the user to combine the two in a process called pan-sharpening, which merges the colour bands with the high-resolution black-and-white imagery. As a result, remote sensing satellites often provide panchromatic (PAN) image with high spatial resolution and multispectral (MS) image with high spectral resolution.

1.6 IMAGE SEGMENTATION

Image segmentation is the process of partitioning a digital image into multiple segments (sets of pixels, also known as super-pixels). The goal of segmentation is to simplify and/or change the representation of an image into something that is more meaningful and easier to analyze. Image segmentation is typically used to locate objects and boundaries (lines, curves, etc.) in images. More precisely, image segmentation is the process of assigning a label to every pixel in an image such that pixels with the same label share certain characteristics. The segmentation is based on measurements taken from the image and might be grey level, colour, texture, depth or motion. The result of image segmentation is a set of segments that collectively cover the entire image, or a set of contours extracted from the image.

Applications of image segmentation include

- Identifying objects in a scene for object-based measurements such as size and shape.
- Identifying objects in a moving scene for object-based video compression (MPEG4).
- Identifying objects which are at different distances from a sensor using depth measurements from a laser range finder enabling path planning for mobile robots.

1.7 IMAGE SEGMENTATION TECHNIQUES

1.7.1 THRESHOLDING

One of the methods widely used for image segmentation. It is useful in discriminating foreground from the background. By selecting an adequate threshold

value T, the gray level image can be converted to binary image. Some of the thresholding techniques are given below,

Mean Technique- This technique used the mean value of the pixels as the threshold value and works well in strict cases of the images that have approximately half to the pixels belonging to the objects and other half to the background.

P-Tile Technique- Uses knowledge about the area size of the desired object to threshold an image.

Histogram Dependent Technique (HDT)- separates the two homogenous region of the object and background of an image.

Edge Maximization Technique (EMT)- Used when there are more than one homogenous region in image or where there is a change of illumination between the object and its background

Visual Technique- Improve people's ability to accurately search for target items.

1.7.2 CLUSTERING

Clustering is defined as the process of identifying groups of similar image primitive. It is a process of organizing the objects into groups based on its attributes. An image can be grouped based on keyword (metadata) or its content (description).

Keyword- Form of font which describes about the image keyword of an image refers to its different features.

Content- Refers to shapes, textures or any other information that can be inherited from the image itself.

1.8 GUIDED IMAGE FILTERING (GIF)

The guided filter performs edge-preserving smoothing on an image, using the content of a second image, called a guidance image, to influence the filtering. The guidance image can be the image itself, a different version of the image, or a completely different image pictured in fig. 1.3. GIF is a neighbourhood operation, like other filtering operations, but takes into account the statistics of a region in the corresponding spatial neighbourhood in the guidance image when calculating the value of the output pixel.

If the guidance is the same as the image to be filtered, the structures are the same—an edge in original image is the same in the guidance image. If the guidance image is different, structures in the guidance image will impact the filtered image, in effect, imprinting these structures on the original image. This effect is called structure transference.

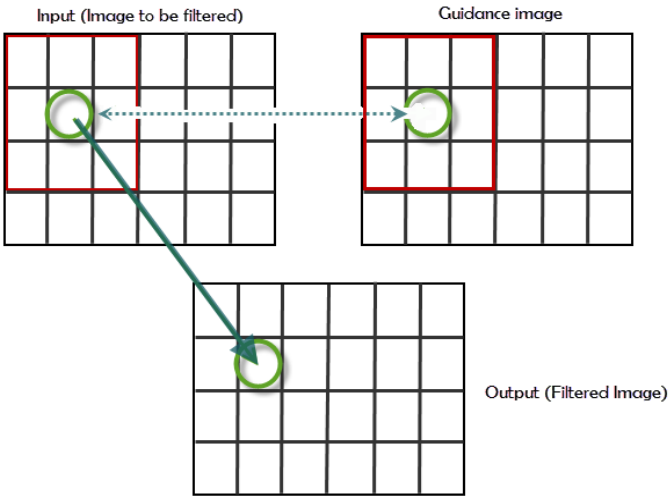

Fig. 1.3. Guided Image Filtering

1.9 FAST GUIDED IMAGE FILTERING (FGIF)

The guided filter is one of several popular algorithms for edge-preserving smoothing. Its time complexity is *O(N)* in the number of pixels N, independent of the filter size. The guided filter can effectively suppress gradient-reversal artifacts and produce visually pleasing edge profiles. Because of these and other properties, the guided filter has been included in official MATLAB 20142 and OpenCV 3.03 and widely adopted in real products.

Despite its popularity and its various third-party implementations, it notices that a simple but significant speedup has not been exploited. This speedup strategy was used for joint upsampling but not for other generic scenarios. This method subsamples the filtering input image and the guidance image, computes the local linear coefficients, and upsamples these coefficients. The upsampled coefficients are adopted on the original guidance image to produce the output. This method reduces the time complexity from *O(N)* to $O(N=s^2)$ for a subsampling ratio *s*. An actual speedup of >10× can be observed.

In this note, the speedup method provides more technical details, visual examples, and publicly**.** This acceleration method is particularly favoured for mega-pixel images, for which the filter size is usually set as proportional to the image size in practice. As such, a local window on the subsampled images can still provide enough pixels for computing local statistics. In extensive real applications for image processing, it was found that this speedup method has almost no visible degradation. Considering the growing usage of the guided filter in real products, this simple speedup will improve the performance of these applications and further popularize this filtering technique.

CHAPTER 2

LITERATURE SURVEY

An image fusion approach based on markov random fields

M. Xu, H. Chen, and P. Varshney

Markov random field (MRF) models are powerful tools to model image characteristics accurately and have been successfully applied to a large number of image processing applications. In this paper the problem of fusion of remote sensing images based on MRF models is investigated. Fusion algorithm under maximum a posteriori criterion is used. It is applicable to both multi-scale decomposition (MD)-based image fusion and non-MD-based image fusion. It is provided to demonstrate the fusion performance improvement.

Here, the image fusion problem is based on a statistical model. This approach is applicable for both non-MD- and MD-based fusion approaches. When the raw source images are directly used for fusion without pre-processing, the fused image can also be modelled as an MRF, and then, the fusion result can be obtained by incorporating a priori Gibbs distribution of the fused image. Visual inspection and quantitative performance evaluation both demonstrate that the employment of the MRF model in the fusion approaches resulted in a better fusion performance than the traditional fusion approaches.

Guided image filtering

K. He, J. Sun, and X. Tang

In this paper, the author proposed a novel explicit image filter called guided filter. Derived from a local linear model, the guided filter computes the filtering output by considering the content of a guidance image, which can be the input image itself or another different image. The guided filter can be used as an edge-preserving smoothing operator like the popular bilateral filter, but it has better behaviours near edges. The guided filter is also a more generic concept beyond smoothing: It can transfer the structures of the guidance image to the filtering output, enabling new filtering applications like de-hazing and guided feathering. Moreover, the guided filter

naturally has a fast and non-approximate linear time algorithm, regardless of the kernel size and the intensity range. Currently, it is one of the fastest edge-preserving filters. Experiments show that the guided filter is both effective and efficient in a great variety of computer vision and computer graphics applications, including edge-aware smoothing, detail enhancement, compression, image matting/feathering, de-hazing, joint up-sampling, etc.

Generalized random walks for fusion of multi-exposure images

R. Shen, I. Cheng, J. Shi, and A. Basu

A single captured image of a real-world scene is usually insufficient to reveal all the details due to under- or over-exposed regions.This problem can be solved by images of the same scene can be first captured under different exposure settings and then combined into a single image using image fusion techniques. The aim is to achieve an optimal balance between two quality measures, i.e., local contrast and color consistency, while combining the scene details revealed under different exposures. A generalized random walks framework is proposed to calculate a globally optimal solution subject to the two quality measures by probability estimation. Experiments demonstrate that this algorithm generates high-quality images at low computational cost. Experimental results demonstrated that this probabilistic fusion produces good results, in which contrast is enhanced and details are preserved with high computational efficiency. Compared to other fusion methods this algorithm produces images with comparable or even better qualities.

Adaptive multi-focus image fusion using a wavelet based statistical sharpness measure

J. Tian and L. Chen

Multi-focus image fusion is to combine a set of images that are captured from the same scene but with different focuses for producing another sharper image. Based on the marginal distribution of the wavelet coefficients is different for images with different focus levels, a new statistical sharpness measure to measure the degree of the image’s blur is proposed. It is evaluated using a locally adaptive Laplacian mixture model. The proposed sharpness measure is then exploited to perform adaptive image

fusion in wavelet domain. The proposed approach could be further extended to be applied in the redundant or complex wavelet domains.

Edge-preserving decompositions for multi-scale tone and detail manipulation

Farbman, R. Fattal, D. Lischinski, and R. Szeliski

The author says that many recent computational photography techniques decompose an image into a piecewise smooth base layer, containing large scale variations in intensity, and a residual detail layer capturing the smaller scale details in the image. It is important to control the spatial scale of the extracted details, desirable to manipulate details at multiple scales, while avoiding visual artifacts. A new way to construct edge-preserving multi-scale image decompositions is given. Current base detail decomposition techniques, based on the bilateral filter, are limited in their ability to extract detail at arbitrary scales. The weighted least squares optimization framework, which is particularly well suited for progressive coarsening of images and for multi-scale detail extraction is described. After describing this operator, it is compared with bilateral filter and other schemes.

Multi-scale contrast manipulation is a valuable digital darkroom technique. Currently it is possible to sharpen images (which may be viewed as increasing the local contrast of the finest scale details), as well as to adjust the global contrast. This does not suffer from some of the drawbacks of bilateral filtering and other previous approaches. Future the smoothness coefficients for the WLS formulation are enhanced further by improving the ability to preserve edge color. While manually adjusting the saturation alleviates the problem, a more principled solution is needed.

Image fusion: Advances in the state of the art

A. A. Goshtasby and S. Nikolov

The author describes that the image fusion is the process of combining information from two or more images of a scene into a single composite image that is more informative and is more suitable for visual perception or computer processing. The objective in image fusion is to reduce uncertainty and minimize redundancy in the output while maximizing relevant information particular to an application or task.

There are several benefits in using image fusion: wider spatial and temporal coverage, decreased uncertainty, improved reliability, and increased robustness of system performance. A single sensor cannot produce a complete representation of a scene. Visible images provide spectral and spatial details, and if a target has the same color and spatial characteristics as its background, it cannot be distinguished from the background. If visible images are fused with thermal images, a target that is warmer or colder than its background can be easily identified, even when its color and spatial details are similar to those of its background. Fused images can provide information that sometimes cannot be observed in the individual input images. Successful image fusion significantly reduces the amount of data to be viewed or processed without significantly reducing the amount of relevant information.

Multifocus image fusion using the non-subsampled contourlet transforms Q. Zhang and B. Guo

A novel image fusion algorithm based on the non-subsampled contourlet transform (NSCT) is proposed in this paper, which aims at solving the fusion problem of multifocus images. Based on the directional vector normal, a 'selecting' scheme combined with the 'averaging' scheme is presented for the low-pass sub-band coefficients. Based on the directional band limited contrast and the directional vector standard deviation, a selection principle is put forward for the band-pass directional sub-band coefficients. It not only extracts more important visual information from source images, but also effectively avoids the introduction of artificial information. It significantly outperforms the traditional discrete wavelet transform-based and the discrete wavelet frame transform-based image fusion methods in terms of both visual quality and objective evaluation, especially when the source images are not perfectly registered.

The NSCT is more suitable for image fusion because of many advantages such as multi-scale, localization, multi-direction, and shift-invariance. Several sets of multi-focus images have been used to evaluate the performance of the proposed fusion algorithm. NSCT- based fusion algorithm performs well in some cases. However, the improved performance is at the cost of increasing computational complexity and

memory during the fusion process. In some cases such as image coding and image compression, where redundancy is a major issue, the higher redundancy of the NSCT may also limit its applications.

A total variation-based algorithm for pixel level image fusion

M. Kumar and S. Dass

In this paper, a total variation (TV) based approach is proposed for pixel-level fusion to fuse images acquired using multiple sensors. Fusion is an inverse problem and a locally affine model is used as the forward model. A TV semi norm based approach in conjunction with principal component analysis is used iteratively to estimate the fused image. The feasibility of the algorithm is demonstrated on images from computed tomography and magnetic resonance imaging as well as visible-band and infrared sensors. It is applied to several different types of datasets. It should focus on analysis of the algorithm performance with additional datasets.

Image Fusion with Guided Filtering

Shutao Li, Xudong Kang, and Jianwen Hu

A fast and effective image fusion method is proposed for creating a highly informative fused image through merging multiple images. The proposed method is based on a two-scale decomposition of an image into a base layer containing large scale variations in intensity, and a detail layer capturing small scale details. A novel guided filtering-based weighted average technique is proposed to make full use of spatial consistency for fusion of the base and detail layers. Experimental results demonstrate that the proposed method can obtain state-of-the-art performance for fusion of multispectral, multifocus, multimodal, and multiexposure images. The proposed method utilizes the average filter to get the two-scale representations, which is simple and effective. The guided filter is used in a novel way to make full use of the strong correlations between neighborhood pixels for weight optimization. Experiments show that the proposed method can well preserve the original and complementary information of multiple input images.

Weighted Guided Image Filtering

Zhengguo Li, Jinghong Zheng, Zijian Zhu, Wei Yao, and Shiqian Wu

In this paper, a weighted guided image filter (WGIF) is introduced by incorporating an edge-aware weighting into an existing guided image filter (GIF) to address the problem. The WGIF inherits advantages of both global and local smoothing filters in the sense that: 1) the complexity of the WGIF is *O(N)* for an image with *N* pixels, which is same as the GIF and 2) the WGIF can avoid halo artifacts like the existing global smoothing filters. The WGIF is applied for single image detail enhancement, single image haze removal, and fusion of differently exposed images. Experimental results show that the resultant algorithms produce images with better visual quality and at the same time halo artifacts can be reduced/ avoided from appearing in the final images with negligible increment on running times.

Fast Guided Filter

Kaiming He and Jian Sun

The guided filter is a technique for edge-aware image filtering. Because of its nice visual quality, fast speed, and ease of implementation, the guided filter has witnessed various applications in real products, such as image editing apps in phones and stereo reconstruction, and has been included in official MATLAB and OpenCV. In this note, it remind that the guided filter can be simply sped up from *O(N)* time to $O(N/s^2)$ time for a subsampling ratio *s*. In a variety of applications, this leads to a speedup of >10× with almost no visible degradation. This acceleration will improve performance of current applications and further popularize this filter.

CHAPTER 3

METHODOLOGY

3.1 INTRODUCTION

In this section, different image segmentation techniques are summarized with emphasis on the K-means clustering, FCM clustering, MFCM clustering, PSO and MPSO segmentation. Clustering is used for image segmentation which is of two types, Hierarchical algorithms and Partitional clustering. Former, uses recursive procedure that computes the present clusters by considering the past clustered sets which is time consuming while the later computes all clusters at once and found to be efficient. Partitional clustering includes K-means, FCM and MFCM clustering. In PSO and MPSO segmentation, Swarm intelligence was used into Artificial intelligence and is used for image segmentation for providing a best outcome. Algorithm of Guided Filter and Fast Guided Filter and its computation was discussed.

3.2 K-MEANS CLUSTERING

K-means clustering is the fast and the simplest algorithm used for image segmentation. Because of its simplicity, it has been widely used in many applications like Pattern recognitions, unsupervised learning of neural network, image processing, Artificial intelligence, machine vision, and many others. It uses the parameter *K* which is to be computed by iteratively performing the partitioning of *N* given sets into *K* clusters (where $K<N$). It works by first calculating the centroids for each sets and then computing the points nearest to the centroids. Euclidean distance is one of the popular methods used for finding distance between the nearest points to the centroids. So, the algorithm aims in minimising the mean square distance between the points and centroids by successive iteration.

Let us consider the image *(i, j)* with pixels *p(i. j)* and c_k be the centroid of k^{th} cluster where *k* is the number of clusters obtained from the image by clustering.

The Euclidean distance, *d* can be calculated by using the formulae,

$$d = \| p(i, j) - c_k \| \quad (1)$$

The new position of the centroid can be calculated as,

$$c_k = \frac{1}{k} \sum_{j \in c_k} \sum_{i \in c_k} p(i, j) \tag{2}$$

The algorithm for K-means clustering is sequenced as follows,

Step1: Initialize number of cluster k and centroid c_k .

Step2: Calculate the Euclidean distance d for each pixel.

Step3: Based on the distance d, assign all the pixels to the nearest centroid.

Step4: Calculate the nearest centroid.

Step5: Repeat the steps until the minimum mean square criteria are satisfied.

Step6: Reshape the pixels of the cluster into image.

Even though *K*-means clustering is found to be very simple, it subject to some of the disadvantages. It requires an appropriate selection of initial centroids to get the desired segmentation result. If it deviates, then the process doesn't provide the better result. It is highly sensitive to noise and outliers. Complexity in *k*-means clustering depends upon the number of iterations and number of clusters.

3.3 FUZZY C MEANS (FCM) CLUSTERING

FCM is the extension of K-means belonging to fuzzy clustering. In hard clustering, each cluster tends to have different data points whereas in fuzzy clustering, two or more clusters can have the same data points. Because of its robust characteristics, it has been wide spread in field of pattern recognition, machine vision, image processing etc. FCM partitions the n data objects x into c fuzzy clusters with y centroids.

Fuzzy clustering is defined in the form of fuzzy matrix as u_{ij} with r rows and c columns. u_{ij}, the element in the i^{th} row and j^{th} column in μ, refers to the membership function of the i^{th} data object with the j^{th} cluster. It aims to minimizing the following expression,

$$F_w = \sum_{j=1}^{c} \sum_{i=1}^{r} u_{ij}^{w} d_{ij} \tag{3}$$

where, $d_{ij} = \| x_i - y_j \|$ is the Euclidean distance between the data objects x_i and the cluster centroids y_j and w (>1) is the weighting exponent.

The centroids of the cluster, y_j is calculated as,

$$y_j = \frac{\sum_{i=1}^{r} u_{ij}^{w} x_i}{\sum_{i=1}^{r} u_{ij}^{w}} \tag{4}$$

The fuzzy membership u_{ij} is updated using the equation,

$$u_{ij} = \frac{\left(\frac{1}{\|x_i - y_j\|} \right)^{\frac{1}{(m-1)}}}{\sum_{j=1}^{n_c} \left(\frac{1}{\|x_i - y_j\|} \right)^{\frac{1}{(m-1)}}} \tag{5}$$

The FCM clustering algorithm is described as follows,

Step1: Initialize membership $U^{(0)} = \left[u_{ij} \right]$ for the data points

Step2: At the k^{th} step, compute the fuzzy centroid $Y^{(k)} = \left[y_i \right]$

Step3: Update the fuzzy membership $U^{k} = \left[u_{ij} \right]$

Step4: If $\|U^{(k)} = U^{(k-1)}\| < \in$, then STOP, else return to step 2

Step5: Determine membership cut-off and compute F_M.

FCM clustering suffers from large computation time where the solution may fall into local optimum. FCM need to specify the number of clusters in prior and also need to determine the value of membership cut-off.

3.4 MODIFIED FUZZY C MEANS (MFCM) CLUSTERING

Usually in an image, the pixels nearby tends to have same characteristics. Therefore, spatial information in an image found to be a highly important criterion which is not satisfied in standard FCM. MFCM overcomes this drawback by giving the significant role to spatial relationship helping in utilizing all the useful information from an image. The relation in (3) can be modified as,

$$F_w = \sum_{j=1}^{c} \sum_{i=1}^{r} u_{ij}^{w} \left\{ d_{ij} + \frac{1}{s_{ik} + 1} \sum_{k \in N_I} \left(\sum_{l=1}^{c} u_{kl} \right)^{w} d_{kj} \right\} \tag{6}$$

where, N_i is the neighbors of pixel i, and s_{ik} is the spatial constraint that influence the pixels i.

The centroid of the cluster, yj is calculated by using (4). The fuzzy membership, u_{ij} is modified as,

$$u_{ij} = \frac{\left(d_{ij} + \frac{1}{s_{ik}+1} \sum_{k \in N_I} \left(\sum_{l=1}^{c} u_{kl} \right)^{w} d_{kj} \right)^{\frac{1}{(m-1)}}}{\sum_{s=1}^{c} \left(d_{is} + \frac{1}{s_{ik}+1} \sum_{k \in N_I} \left(\sum_{l=1}^{c} u_{kl} \right)^{w} d_{kj} \right)^{\frac{1}{(m-1)}}} \quad (7)$$

The algorithm for MFCM is sequenced as follows [26],

Step1: Fix the value of *c*, *r* and let ε be the positive constant.

Step2: Estimate the initial value of centroid, y_j.

Step3: Obtain the fuzzy membership function, u_{ij} using (7).

Step4: Update the value of the centroid, y_j using (4).

Step5: Repeat the steps 3 and 4 until it satisfies the relation (6).

Even though it considers the spatial consistency of an image, it provides the same or little variations from the traditional FCM algorithm under several iterations in minimizing the membership function.

3.5 PARTICLE SWARM OPTIMIZATION (PSO) SEGMENTATION

"Swarm intelligence (SI) is artificial intelligence based on the collective behaviour of decentralized, self-organized systems"[definition]. One of such is Particle swarm Optimization is the population based Optimization algorithm. Here the concept is based on the behaviour of group of flocking birds searching for food in a defined area. Swarm of n individuals shares the information with each other either directly or indirectly to find the food quicker. This concept is used in image segmentation and proved to give best results than the other techniques.

In a given population, particles are randomly distributed in the search space, each having different intensities and positions. During flight, the particle tends to update their intensity and position based upon the fitness value to reach the optimum solution. Two optimum solutions describe the fitness function. They are pbest solution and gbest solution. Former refers to the best solution achieved by each particle and the later refers to best solution achieved by the particle among the entire population.

After finding the two best values, the particle updates its velocity and position with the help of the following equation,

$$p[\ ] = p[\ ] + f1 * r(\ ) * \left(pbest[\ ] - pcur[\ ]\right) + f2 * r(\ ) * \left(gbest[\ ] - pcur[\ ]\right) \quad (8)$$

$$cur[\ ] = cur[\ ] + p[\ ] \quad (9)$$

where, p[ ] is the particle velocity, cur[ ] is the cur particle (solution), r( ) is a random number between 0 and 1. f1, f2 are learning factors.

The algorithm for PSO based segmentation is listed as follows,

Step 1: Read the input image to be segmented.

Step 2: Select PSO method to be applied on that image with a particular threshold level.

Step 3: For each particle in the population update particle's fitness in the search space and update particle's best in the search space, then move the particle in the population.

Step 4: For each particle, if swarm gets better then extend the swarm/particle life.

Step 5: For each particle, if swarm is not improving its performance then reduce the swarm life.

Step 6: The swarm is considered for next iteration.

Step 7: The failed swarms are deleted.

Step 8: Reset threshold counter.

One of the key issues in designing the successful PSO image segmentation is the representation step ie., finding the suitable mapping between a particle and PSO particles. But it tends to provide better segmentation results by iteratively performing the operation.

3.6 MODIFIED PARTICLE SWARM OPTIMIZATION (MPSO) SEGMENTATION

MPSO is the extended form of PSO where the important issue in fitness function is solved by employing it with some clustering criteria. In MPSO, the inertia weight, *w* is incorporated in equation (8) as,

$$p[\ ] = w * p[\ ] + f1 * r(\ ) * \left(pbest[\ ] - pcur[\ ]\right) + f2 * r(\ ) * \left(gbest[\ ] - pcurrent[\ ]\right) \quad (10)$$

$$w = \left(w_1 - w_2\right) * \frac{\left(m_i - i\right)}{m_i} + w_2 \quad (11)$$

where, ω_1 and ω_2 are the initial and final values of the inertia weight, respectively, m_i is the maximum number of iterations, and i is the current iteration number. In addition to that the two constants, f_1 and f_2, in the PSO algorithm, are modified as,

$$f_1 = \left(f_{1i} - f_{1f}\right) \times \frac{m_i}{i} + f_{1i} \tag{12}$$

$$f_2 = \left(f_{2i} - f_{2f}\right) \times \frac{m_i}{i} + f_{2i} \tag{13}$$

where, f_{1i} and f_{1f} represent the initial and final values of f_1, respectively, and f_{2i} and f_{2f} represent the initial and final values of f_2, respectively.

The algorithm for MPSO based segmentation is listed as follows [28],

Step 1: Initiate the parameters of each particle, including its position and velocity.

Step 2: Update the velocity and position of each particle by (10) and (11), respectively.

Step 3: For each particle in the population update particle's fitness in the search space and update particle's best in the search space, then move the particle in the population.

Step 4: Update pbest of each particle and gbest.

Step 5: Stop if the current optimization solution is good enough or some stopping criterion is satisfied. Otherwise, go to Step 2.

It has been seen that PSO is an off-line optimization algorithm that is suitable for solving a complex problem with approximate solutions at low cost.

3.7 GUIDED IMAGE FILTERING (GIF) COMPUTATION

The guided filter assumes that the filtering output O is a linear transformation of the guidance image I in a local window ω_k centered at pixel k.

$$O_{i=a_k I_i + b_k \; \forall i \epsilon \omega_k} \tag{14}$$

where ω_k is a square window of size $(2r+1)\times(2r+1)$.

The linear coefficients a_k and b_k are constant in ω_k and can be estimated by minimizing the squared difference between the output image O and the input image P.

$$E(a_k, b_k) = \sum_{i \in \omega_k} ((a_k I_i + b_k - P_i)^2 + \epsilon a_2^k) \tag{15}$$

where ϵ is a regularization parameter given by the user.

The coefficients a_k and b_k can be directly solved by linear regression equation as follows:

$$a_k = \frac{\frac{1}{|\omega|}\sum_{i\in\omega_k}(I_i P_i - \mu_k P'_k)}{\delta k + \epsilon} \tag{16}$$

$$b_k = P'_k - a_k\,\mu_k \tag{17}$$

where, μ_k and δ_k are the mean and variance of I in ω_k respectively, $|\omega|$ is the number of pixels in ω_k, and P_k is the mean of P in ω_k. Next, the output image can be calculated according to (14).

As shown in fig. 3.1, all local windows centered at pixel k in the window P_i will contain pixel i. So, the value of O_i in (14) will change when it is computed in different windows,ω_k. To solve this problem, all the possible values of coefficients $a_k$and b_k are first averaged. Then, the filtering output is estimated as follows:

$$O_i = a'_i I_i + b'_i \tag{18}$$

where $a'_i = \frac{1}{|\omega|}\sum_{k\in\omega_i}(a_k), b'_i = \frac{1}{|\omega|}\sum_{k\in\omega_i}(b_k)$. In this paper, $G_{r,\epsilon}(P, I)$ is used to represent the guided filtering operation, where r and ϵ are the parameters which decide the filter size and blur degree of the guided filter, respectively. Moreover, P and I is the input image and guidance image, respectively.

Furthermore, when the input is a color image, the filtering output can be obtained by conducting the guided filtering on the red, green, and blue channels of the input image, respectively. And when the guidance image I is a color image, the guided filter should be extended by the following steps.

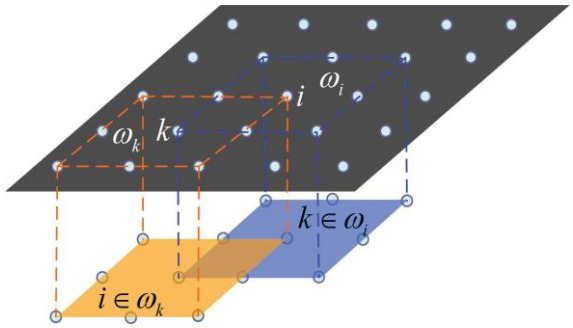

Fig. 3.1. Window Choice

First, equation (14) is rewritten as follows:

$$O_{i=a_k^T I_i + b_k \, \forall i \epsilon \omega_k} \tag{19}$$

where, a_k is a 3 × 1 coefficient vector and I_i is a 3 × 1 color vector.

Then, similar to (3.3)–(3.5), the output of guided filtering can be calculated as follows:

$$a_k = (\sum_k + \epsilon U)(\frac{1}{|\omega|} \sum_{i \in \omega_k} (I_i P_i - \mu_k p'_k)) \tag{20}$$

$$b_k = P'_k - a_k{}^T \mu_k \tag{21}$$

$$O_i = a'_i{}^T I_i + b'_i \tag{22}$$

where $\sum_k$ is the 3×3 covariance matrix of **I** in ω_k, and *U* is the 3 × 3 identity matrix. Computational complexity of GIF is *O(N)* where N is the number of pixels.

3.8 ALGORITHM FOR GIF AND FGIF

Algorithm I shows the pseudo-code of the guided filter, where f_{mean} *(.; r)* denotes a mean filter with a radius r. In the above, a´ and b´ in (22) are two smoothed maps, and the edges and structures in q are mainly given by modulating the image I (thus called guidance). But the major computation of guided filter is for the smoothed maps of a´ and b´, which need not be performed in full-resolution.

Algorithm II describes the subsampled version for Fast Guided Filter. We subsample (nearest-neighbour or bilinear) the input p and the guidance I by a ratio s. All the box filters are performed on the low-resolution maps, which are the major computation of the guided filter.

The two coefficient maps a´ and b´ are bilinearly upsampled to the original size. Finally, the output q is still computed by q = a´I +b´. In this last step, the image I is the full-resolution guidance that is not downsampled, and it will still faithfully guide the output.

I. Algorithm for Guided Filter

1. $mean_I = f_{mean}(I, r)$
   $mean_p = f_{mean}(p, r)$
   $corr_I = f_{mean}(I.* I, r)$
   $corr_{Ip} = f_{mean}(I.* p, r)$
2. $var_I = corr_I - mean_I. * mean_I$
   $cov_{Ip} = corr_{Ip} - mean_I. * mean_p$
3. $a = cov_{Ip} ./ (var_I + \in)$
   $b = mean_p - a. * mean_I$
4. $mean_a = f_{mean}(a, r)$
   $mean_b = f_{mean}(b, r)$
5. $q = mean_a. * I + mean_b$

II. Algorithm for Fast Guided Filter

1. $I' = f_{subsample}(I, s)$
   $p' = f_{subsample}(p, s)$
   $r' = r/s$
2. $mean_I = f_{mean}(I', r)$
   $mean_p = f_{mean}(p', r)$
   $corr_I = f_{mean}(I'.* I', r)$
   $corr_{Ip} = f_{mean}(I'.* p', r)$
3. $var_I = corr_I - mean_I. * mean_I$
   $cov_{Ip} = corr_{Ip} - mean_I. * mean_p$
4. $a = cov_{Ip} ./ (var_I + \in)$
   $b = mean_p - a. * mean_I$
5. $mean_a = f_{mean}(a, r)$
   $mean_b = f_{mean}(b, r)$
6. $mean_a = f_{subsample}(mean_a , s)$
   $mean_b = f_{subsample}(mean_b , s)$
7. $q = mean_a. * I + mean_b$

The computation of all box filters reduces from $O(N)$ complexity to $O(N/s^2)$. The last bilinear upsampling and output steps are $O(N)$ complex, but only take a small fraction of overall computation .

3.9 BLOCK DIAGRAM

Fig. 3.2 shows the proposed image fusion method based on segmentation techniques. First, Gaussian filter is used to get the two-scale representation. Then, the base and the detail layers undergo fusion through using weighted guided image filtering (WGIF). Image segmentation is used for saliency map construction.

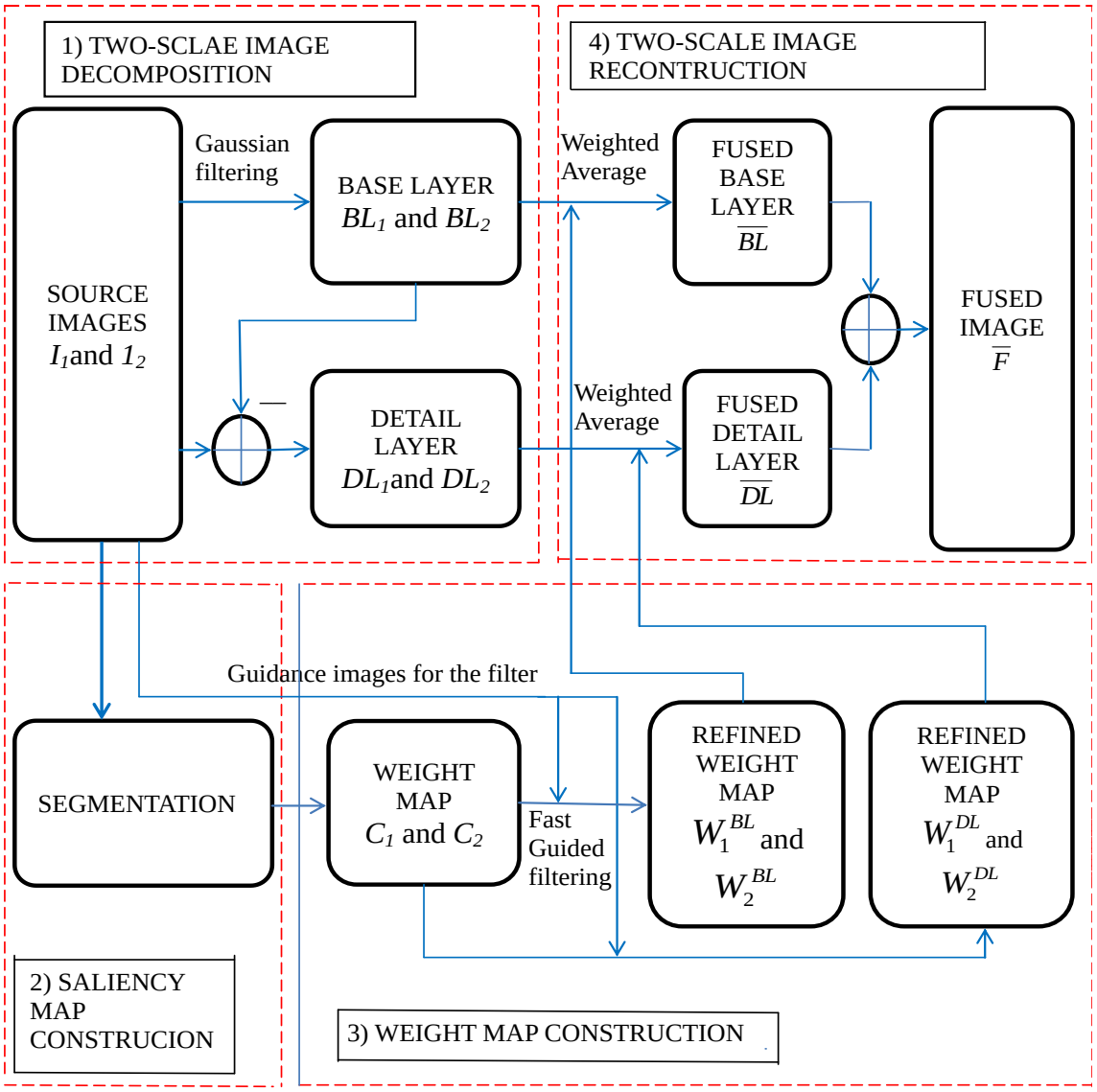

Fig. 3.2. Block Diagram

3.9.1. TWO-SCALE IMAGE DECOMPOSITION

Two or more source images are taken which are co-registered to perform fusion in an effective way. These source images undergo two-scale decomposition by using gaussian filtering. Two-scale decomposition divides the large and the small details of the image as base and detail layers respectively.

The base layer of each source image is attained by,

$$BL_n = I_n * G \tag{23}$$

where, BL_n is the n^{th} base layer, I_n is the n^{th} source image and G is the Gaussian filter.

Then, the detail layer can be attained easily by subtracting the source image and the base layer.

$$DL_n = I_n - BL_n \tag{24}$$

3.9.2. SALIENCY MAP CONSTRUCTION

Saliency map construction normally by a filter is usually noisy and results in artifacts in the fused image. Using segmentation is the effective way to overcome this problem which classifies the image into several groups of dissimilar characteristics, making it more meaningful that helps in constructing the weight maps further. In this paper, Segmentation technique is proposed to apply on the source images to get the saliency map to reduce noise and to produce a better quality fused image.

$$SM_n = I_n * segmentation \tag{25}$$

where, SM_n is the saliency map of the n^{th} image.

Here, segmentation techniques like K-means, FCM and PSO was applied to the source images and the results are analysed. The motivation of the proposed saliency map construction is that if the pixel *N* is in the flat area of the guidance image then its variance is small and if it is in the edge area then its variance is very large. This signifies the concept of segmentation by dividing the intensities of the image into small and large scale variations. The computed saliency map gives the detailed information for further steps.

3.9.3. WEIGHT MAP CONSTRUCTION

Saliency comparison is done to identify the weight maps. Saliency comparison denotes that adjacent pixels having similar intensity or colour are assigned with the similar weights.

Weight maps are determined by

$$C_n^N = \begin{cases} 1 if\ S_n^N = max\left(S_1^N, S_2^N, \ldots S_K^N\right) \\ 0 \qquad\qquad otherwise \end{cases} \tag{26}$$

where, *K* is the number of source images, $S_n{}^N$ is the saliency value of the pixel *N* in the n^{th} image.

Each weight map C_n is then given to the weighted guided image filtering with I_n as the guidance image.

$$W_n^{BL} = G_{x_1,y_1}\left(C_N, I_n\right) \tag{27}$$

$$W_n^{DL} = G_{x_2,y_2}\left(C_N, I_n\right) \tag{28}$$

where, x_1,x_2, y_1 and y_2 are the parameters of the guided filter, W_n^{BL} and W_n^{DL} are the weights maps of base and the detail layer respectively.

3.9.4. TWO-SCALE IMAGE RECONSTRUCTION

Two-scale reconstruction is the final step to get the fused image. This can be done by fusing the base and the detail layers of the source images. Here, weighted averaging is used for fusing.

Relation is given by,

$$BL_F = \sum_{n=1}^{K} W_n^{BL} BL_n \tag{29}$$

$$DL_F = \sum_{n=1}^{K} W_n^{DL} DL_n \tag{30}$$

where, BL_F is the fused base layer and DL_F is the fused detail layer.

Then, the resultant fused image F can be derived by just adding BL_F and DL_F.

$$F = BL_F + DL_F \tag{31}$$

CHAPTER 4

SIMULATION RESULTS

The results of segmentation based satellite image fusion method on MS and PAN images using fast guided filter are presented in this chapter. The performance metrics that has been used to analyse the results are Mean Square Error (*MSE*), Peak Signal to Noise Ratio (*PSNR*), Average Difference (*AD*), Structural Content (*SC*), Normalized Cross Correlation (*NK*), Normalized Absolute Error (NAE), and Structural Similarity Index Measure (SSIM). Elapsed time is computed for comparing the complexity of guided and fast guided filter and the results have been shown. The images were analysed and processed in MATLAB. Ikonos and QuickBird satellite images are used here.

4.1 RESULTS

4.1.1 INPUT IMAGES OF IKONOS SENSOR

Ikonos is a commercial earth observation satellite, and was the first to collect publicly available high resolution imagery at 1 and 4 meter resolution. It offers multispectral (MS) and panchromatic (PAN) imagery. The Ikonos launch was called "one of the most significant developments in the history of the space age". Spatial resolution of the sensor is 0.8 m for panchromatic (1m PAN) and 4 meter for multispectral (4m MS). Spectral resolution of Ikonos sensor is given in Table 4.1.

TABLE 4.1. Spectral Resolution of Ikonos Sensor

Band	**Wavelength Region(μm)**
1	0.45-0.52 (blue)
2	0.52-0.60(green)
3	0.63-0.69(red)
4	0.76-0.90(nearIR)
PAN	0.45-0.90(PAN)

The input images (panchromatic and multispectral) from the Ikonos sensor are shown as in fig. 4.1.

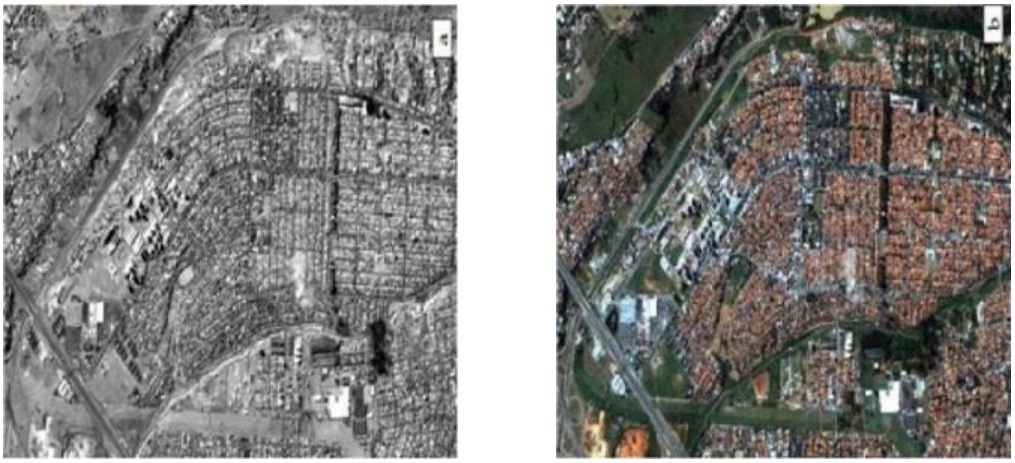

(a) (b)

Fig. 4.1. Panchromatic and Multispectral Images of Ikonos Sensor

4.1.2 INPUT IMAGES OF QUICKBIRD SENSOR

QuickBird was a high resolution commercial earth observation satellite, owned by Digital Globe. QuickBird used Ball Aerospace's Global Imaging System 2000 (BGIS 2000). The satellite was initially expected to collect at 1 meter resolution. The satellite collected panchromatic (black and white) imagery at 61 centimeter resolution and multispectral imagery at 2.44 (at 450 km) to 1.63meter (at 300km) resolution, as orbit altitude is lowered during the end of mission life. At this resolution, detail such as buildings and other infrastructure are easily visible. The imagery can be can be used in mapping applications, such as Google Earth and Google Maps. Spectral resolution of QuickBird sensor is given in Table 4.2.

TABLE 4.2. Spectral Resolution of QuickBird Sensor

Band	**Wavelength Region(nm)**
1	430 - 545 (blue)
2	466 - 620 (green)
3	590 - 710 (red)
4	715 - 918 (nearIR)
PAN	405 - 1053 (PAN)

The input images (panchromatic and multispectral) from the QuickBird sensor are shown as in fig. 4.2.

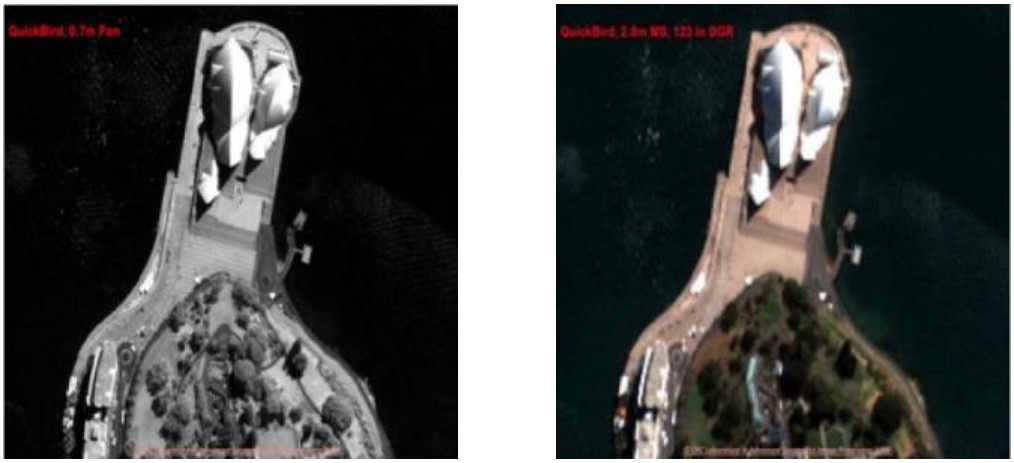

(a) (b)

Fig. 4.2. Panchromatic and Multispectral Images of QuickBird Sensor

4.2 QUALITY METRICS FOR PERFORMANCE EVALUATION

Many parameters are used for analysing the quality of image fusion. They can be qualitative or quantitative analysis. Qualitative analysis deals with measuring the performance of the fused image by visual comparison of the fused image and the input images and quantitative analysis deals with measuring the performance of the fused image by two (with reference image and without reference image). The following seven quality metrics was used for comparison.

A. Mean Squared Error (MSE): MSE is the most often used, full-reference image quality metric and is defined as,

$$MSE = \frac{1}{MN}\sum_{i=1}^{M}\sum_{j=1}^{N}\left(R(i,j)-F(i,j)\right)^2 \tag{32}$$

where, *R(i, j)* is the reference image, *F(i, j)* is the fused image to be assessed, *i* is pixel row index, *j* is pixel column index, and *M*, *N* are number of rows and columns.

B. Peak signal to noise ratio (PSNR): PSNR is obtained by just dividing the number of gray levels in the image by the *MSE*. The *PSNR* measure is given by,

$$PSNR = 10\log_{10}\frac{255^2}{MSE} \tag{33}$$

C. Average Difference (AD): AD is simply the average of difference between the reference signal and fused image. It is given by the equation,

$$AD = \frac{1}{MN}\sum_{i=1}^{M}\sum_{j=1}^{N}\left(R(i,j) - F(i,j)\right) \tag{34}$$

D. Structural Content (SC): SC is also correlation based measure and measures the similarity between two images. *SC* is given by the equation,

$$SC = \frac{\sum_{i=1}^{M}\sum_{j=1}^{N}\left(F(i,j)\right)^2}{\sum_{i=1}^{M}\sum_{j=1}^{N}\left(R(i,j)\right)^2} \tag{35}$$

E. Normalized Cross Correlation (NK): NK is used to find out similarities between fused image and registered image and it is given by the following equation,

$$NK = \frac{\sum_{i=1}^{M}\sum_{j=1}^{N}\left(R(i,j) * F(i,j)\right)}{\sum_{i=1}^{M}\sum_{j=1}^{N}\left(R(i,j)\right)^2} \tag{36}$$

F. Normalized absolute error (NAE): The large value of *NAE* means that image is poor quality. *NAE* is defined as follows,

$$NAE = \frac{\sum_{i=1}^{m}\sum_{j=1}^{n}\left(\left|R(i,j) - F(i,j)\right|\right)}{\sum_{i=1}^{m}\sum_{j=1}^{n}\left(R(i,j)\right)} \tag{37}$$

G. Structural Similarity Index Measure (SSIM): SSIM is the metric used to identify the range of similarity between the images. The SSIM index is a decimal value between 0 and 1 and it should be high (near to 1). The definition for SSIM is,

$$SSIM = \frac{\left(2\mu_x\mu_y + c_1\right)\left(2\sigma_{xy} + c_2\right)}{\left(\mu_x^2 + \mu_y^2 + c_1\right)\left(\sigma_x^2 + \sigma_y^2 + c_2\right)} \tag{38}$$

where, $\mu_x$is the average of x, $\mu_y$is the average of y, ${\sigma_x}^2$ is the variance of x, ${\sigma_y}^2$ is the variance of y, σ_{xy} is the covariance of x and y and c_1 and c_2 are two variables to stabilize the division with weak denominator.

4.3 COMPARISON OF VARIOUS SEGMENTATION ALGORITHMS

Proposed algorithm was experimented with five segmentation techniques that include K-means clustering, FCM clustering , Modified FCM clustering, PSO and MPSO segmentation on two pairs of input images (Ikonos and QuickBird) shown in fig. 4.1 and fig. 4.2 and their metrics have been evaluated. The PAN and the MS images taken for evaluation are co-registered (process of transforming different sets of data into one coordinate system. Data may be multiple photographs, data from different sensors, times, depths, or viewpoints).

(a) Without Segmentation

(b) K-means

(c) FCM

(d) MFCM

(e) PSO

(f) MPSO

Fig. 4.3. Fusion results of proposed method without and with different segmentation techniques for the input images in fig. 4.1.

TABLE 4.3. Quality metrics corresponding to six fusion results in fig. 4.3.

	MSE	**PSNR**	**AD**	**SC**	**NK**	**NAE**	**SSIM**
Without segmentation	0.1891	62.595	-0.0666	0.8416	0.8326	16.0000	0.0729
K-MEANS	0.0622	72.2536	-0.0341	0.9952	0.9985	3.6600	0.9104
FCM	0.0621	72.2622	-0.0339	0.9955	0.9986	3.6503	0.9107
MFCM	0.0621	72.2634	-0.0339	0.9953	0.9986	3.6502	0.9107
PSO	0.0616	72.3405	-0.033	0.8785	0.9292	3.5500	0.9039
MPSO	0.0615	72.3413	-0.0329	0.8790	0.9294	3.5411	0.9039

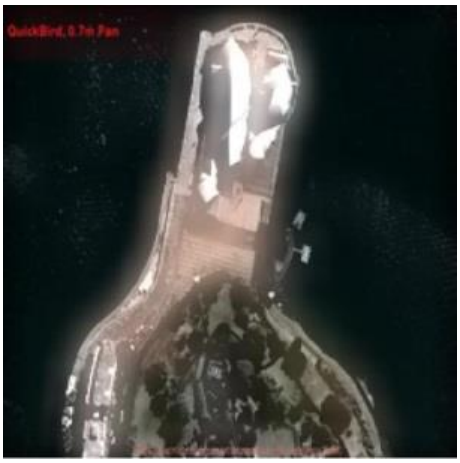

(a) Without Segmentation

(b) K-means

(c) FCM

(d) MFCM

(e) PSO

(f) MPSO

Fig. 4.4. Fusion results of proposed method without and with different segmentation techniques for the input images in fig. 4.2.

TABLE 4.4. Quality metrics corresponding to six fusion results in fig. 4.4.

	MSE	**PSNR**	**AD**	**SC**	**NK**	**NAE**	**SSIM**
Without segmentation	0.1025	67.9139	-0.0415	0.8078	0.8551	13.0000	0.2347
K-MEANS	0.0273	79.4065	-0.0104	0.9406	0.9710	2.2392	0.9727
FCM	0.0273	79.4126	-0.0091	0.9845	0.9718	1.9701	0.9748
MFCM	0.0271	79.4722	-0.0088	0.9722	0.9871	1.9007	0.9752
PSO	0.0268	79.5455	-0.0084	0.9387	0.9655	1.8192	0.8962
MPSO	0.0267	79.5476	-0.0084	0.9388	0.9655	1.8185	0.8964

Fig. 4.3 and Fig. 4.4 show the outcome of the image fusion of PAN and MS image of Ikonos and QuickBird sensor respectively. The image (a) in both fig. 4.3 and fig. 4.4 are the results obtained without any segmentation techniques whereas images (b), (c), (d), (e) and (f) are the results of our proposed algorithm where (b) corresponds to K-means, (c) FCM, (d) MFCM, (e) PSO and (f) the result of MPSO segmentation. Quality metrics corresponding to the fusion results of fig. 4.3 and fig. 4.4 is tabulated in Table 4.3 and Table 4.4.

From the table, it infers that the fused image shows better results when segmentation is applied. Without segmentation, the main quality factors *MSE* and *PSNR* failed to meet the desired criteria whereas with segmentation, it shows best results with low MSE and high PSNR and also with other evaluation metrics (*AD, SC, NK, NAE, SSIM*) proving that the proposed algorithm works well in image fusion. PSNR is given in db. FCM found to be more efficient than K-means even though the computation time is lesser for K-means. Among the segmentation techniques, MPSO segmentation proved to be best in fusion process with lower value of *MSE* and higher value of *PSNR*. The performance ranges from MPSO to PSO, PSO to MFCM, MFCM to FCM, and FCM to K-means (high to low). K-means found to be least in performance.

4.4 COMPARISON OF GUIDED AND FAST GUIDED FILTER

Comparison of guided and fast guided filter has been done by computing the time complexity for different algorithms. The elapsed time taken by different algorithms is represented as bar graph in fig. 4.5 for Ikonos images and in fig. 4.6 for Quickbird images. It will be seen that the time taken for the different algorithms with fast guided filter is lesser than the one with the guided filter. In practice, it has been observed a speedup of >10× when s = 4. Thus, the time complexity has been reduced by using fast guided filter thereby reducing the computation complexity from $O(N)$ to $O(N/s^2)$. Here, the sampling ratio of 4 has been implemented to enhance the image quality.

Among the segmentation algorithms implemented in the proposed method, MPSO proves to have better performance with less error and high PSNR. Experiments

has been carried out based on MPSO segmentation algorithm with different sampling ratios (s = 1 to 10) using guided and fast guided filter. From the fig. 4.7 and fig. 4.8, it depicts that the time taken for the guided filter is high than the fast guided filter. It shows that when the sampling ratio increases, the elapsed time increases.

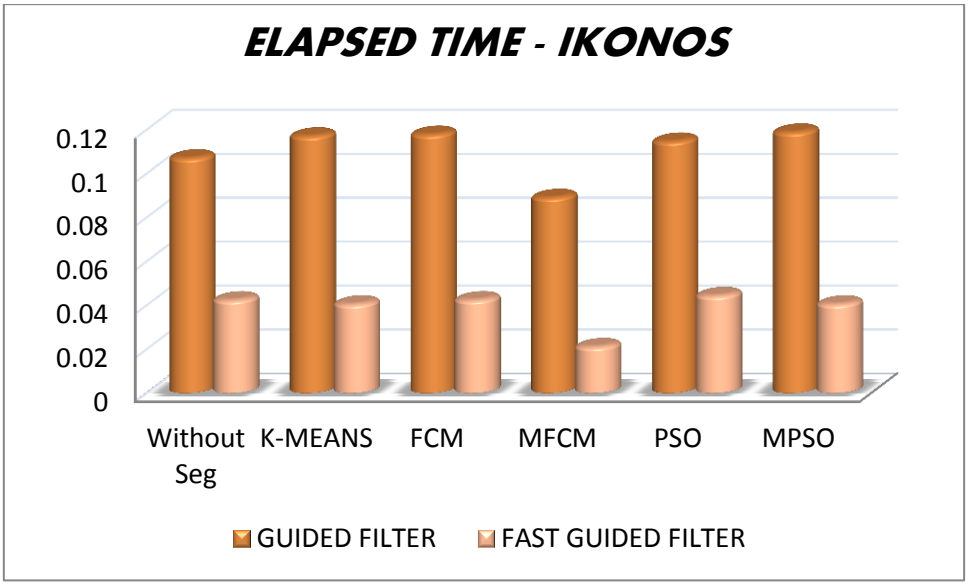

Fig. 4.5. Bar Graph representation of the elapsed time taken by different segmentation algorithms using guided and fast guided filter applied on Ikonos images.

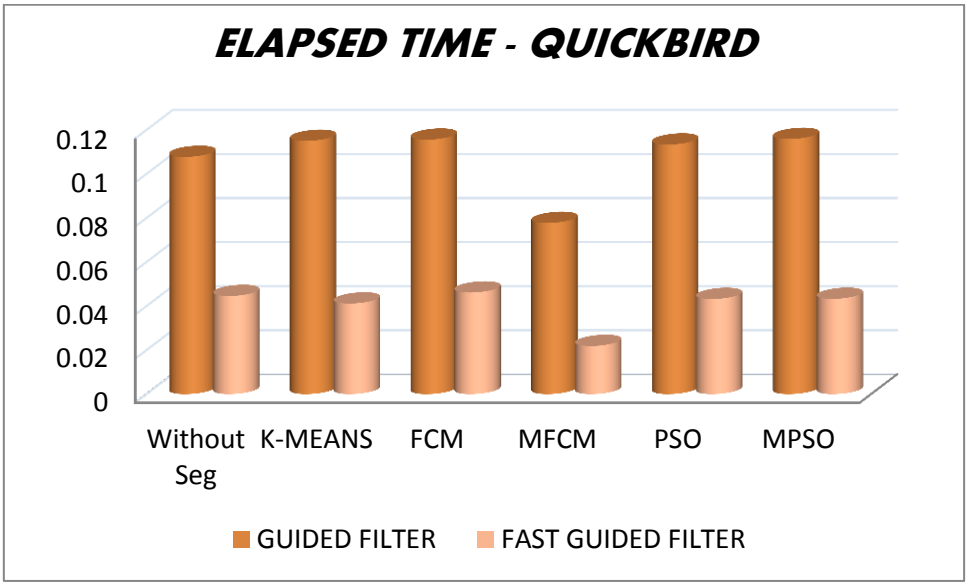

Fig. 4.6. Bar Graph representation of the elapsed time taken by different segmentation algorithms using guided and fast guided filter applied on QuickBird images.

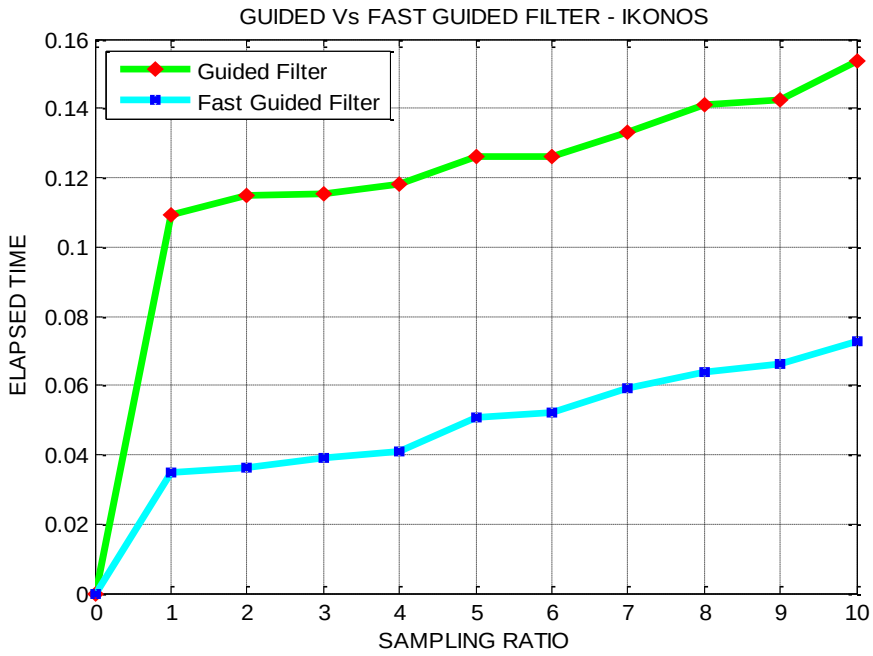

Fig. 4.7. Elapsed time for different sampling ratios (s= 1 to 10) based on MPSO segmentation applied on Ikonos images

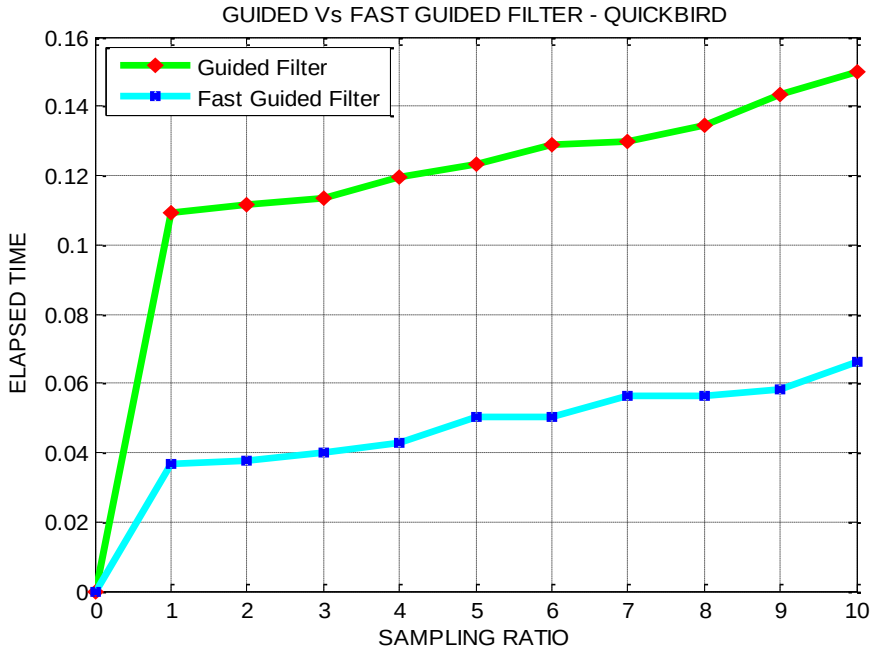

Fig. 4.8. Elapsed time for different sampling ratios (s= 1 to 10) based on MPSO segmentation applied on QuickBird images.

INFERENCE: Computational Complexity has been reduced by using fast guided filter with lesser time and space complexity.

CHAPTER 5

CONCLUSION AND FUTURE WORK

A novel image fusion technique is proposed using image segmentation which can be used in several applications in image processing mainly in the field of remote sensing. Image segmentation plays a major role in our algorithm helping in providing a desired outcome. Bringing swarm intelligence into image segmentation had come out with good result than the other techniques, Experimental results demonstrated proves that our algorithm is effective than other fusion methods.

In future, the fusion architecture can be implemented on FPGA with low power, reduced area and high performance. This fusion process can also be further extended by using other optimization based segmentation techniques.

REFERENCES

[1] A. A. Goshtasby and S. Nikolov, “Image fusion: Advances in the state of the art,” *Inf. Fusion*, vol. 8, no. 2, pp. 114–118, Apr. 2007.

[2] Hassan Ghassemian, “A review of remote sensing image fusion methods,” Information Fusion, vol. 32, pp. 75-89, 2016.

[3] D. Looney and D. Mandic, “Multiscale image fusion using complex extensions of EMD,” *IEEE Trans. Signal Process.*, vol. 57, no. 4, pp. 1626–1630, Apr. 2009.

[4] G. Piella, “Image fusion for enhanced visualization: A variational approach,” *Int. J. Comput. Vision*, vol. 83, pp. 1–11, Jun. 2009.

[5] J. Liang, Y. He, D. Liu, and X. Zeng, “Image fusion using higher order singular value decomposition,” *IEEE Trans. Image Process.*, vol. 21, no. 5, pp. 2898–2909, May 2012.

[6] P. Burt and E. Adelson, “The laplacian pyramid as a compact image code,” *IEEE Trans. Commun.*, vol. 31, no. 4, pp. 532–540, Apr. 1983.

[7] M. Xu, H. Chen, and P. Varshney, “An image fusion approach based on markov random fields,” *IEEE Trans. Geosci. Remote Sens.*, vol. 49, no. 12, pp. 5116–5127, Dec. 2011.

[8] Kaiming He, Jian Sun, and Xiaoou Tang, “Guided Image Filtering,” *IEEE Trans. Pattern Analysis and Machine Intelligence*, vol. 35, no. 6, June 2013.

[9] Shutao Li, Xudong Kang, and Jianwen Hu, “Image Fusion with Guided Filtering,” *IEEE trans. image process., vol. 22, no. 7, July 2013.*

[10] C. Tomasi and R. Manduchi, “Bilateral filtering for gray and color images,” in *Proc. IEEE Int. Conf. Comput. Vis.*, pp. 836–846, Jan. 1998.

[11] P. Choudhury and J. Tumblin, “The trilateral filter for high contrast images and meshes,” in *Proc. Eurograph. Symp. Rendering*, pp. 186–196, 2003.

[12] B. Y. Zhang and J. P. Allebach, “Adaptive bilateral filter for sharpness enhancement and noise removal,” *IEEE Trans. Image Process.*, vol. 17, no. 5, pp. 664–678, May 2008.

[13] C. C. Pham, S. V. U. Ha, and J. W. Jeon, "Adaptive guided image filtering for sharpness enhancement and noise reduction," in *Advances in Image and Video Technology*, Berlin, Germany: Springer-Verlag, 2012.

[14] Zhengguo Li, Jinghong Zheng, Zijian Zhu, Wei Yao, and Shiqian Wu, "Weighted Guided Image Filtering," *IEEE trans. Image process.*, vol. 24, no. 1, Jan. 2015.

[15] Arti Taneja, Dr. Priya Ranjan, and Dr. Amit Ujjlayan, "A Performance Study of Image Segmentation Techniques," in *4th International Conference on Reliability, Infocom Technologies and Optimization (ICRITO) (Trends and Future Directions)*, Sep. 2015.

[16] Akanksha Bali, and Dr. Shailendra Narayan Singh, "A Review on the Strategies and Techniques of image Segmentation," in *5th International Conference on Advanced Computing & Communication Technologies*, 2015.

[17] A. K. Jain, M. N. Murty, and P. J. Flynn, "Data Clustering: A Review," in *ACM Computing Surveys*, vol. 31, no. 3, Sep. 1999.

[18] S. Saraswathi, and Dr. A. Allirani, "Survey on Image Segmentation via Clustering," in *International Conference on Information Communication and Embedded Systems (ICICES)*, 2013.

[19] Chinki Chandhok, Soni Chaturvedi,and Dr.A.A Khurshid, "An Approach to Image Segmentation using K-means Clustering Algorithm," *International Journal of Information Technology (IJIT)*, vol. 1, no.1, Aug. 2012.

[20] P. Srinivasa Rao, K. Suresh, and B. Ravi Kiran, "Image Segmentation using Clustering Algorithms," in *International Journal of Computer Applications*, vol. 120, no.14, June 2015.

[21] Samina Naz, Hammad Majeed, and Humayun Irshad, "Image Segmentation using Fuzzy Clustering: A Survey," in *6th International Conference on Emerging Technologies (ICET)*, 2010.

[22] Abhay Sharma, Rekha Chaturvedi, and Dr. Umesh Kr. Dwivedi, " Recent Trends and Techniques in Image Segmentation using Particle Swarm Optimization-a Survey*," International Journal of Scientific and Research Publications*, vol. 5, Issue 6, June 2015.

[23] Zhong Qu and Tengfei Gao, “Research on Image Segmentation Based on Global Optimization Search Algorithm,” in *7th International Conference on Fuzzy Systems and Knowledge Discovery (FSKD)*, 2010.

[24] Nameirakpam Dhanachandra, Khumanthem Manglem and Yambem Jina Chanu, “Image Segmentation using *K*-means Clustering Algorithm and Subtractive Clustering Algorithm,” in *11th International Multi-Conference on Information Processing (IMCIP)*, 2015.

[25] A. K. Saritha, and P. M. Ameera, “Image segmentation based on kernel fuzzy C means clustering using edge detection method on noisy images,” *International Journal of Advanced Research in Computer Engineering & Technology (IJARCET)*, vol. 2, Issue 2, Feb. 2013.

[26] Anita Tandan, Rohit Raja, and Yamini Chouhan, “Image Segmentation Based on Particle Swarm Optimization Technique,” *International Journal of Science, Engineering and Technology Research (IJSETR)*, vol. 3, Issue 2, Feb. 2014.

[27] Kaiming He, and Jian Sun, “Fast Guided Filter,” *Computer Vision and Pattern Recognition*, Cornell University Library, arXiv:1505.00996**,** 5 May 2015.

[28] P. Jagalingam and Arkal Vittal Hegde, “A Review of Quality Metrics for Fused Image,” *International conference on water resources, coastal and ocean engineering (ICWRCOE)*, 2015.

LIST OF PUBLICATIONS

Conferences

- Presented a paper titled "Satellite Image Fusion using Clustering Algorithms" in ICMR sponsored *IEEE International Conference on Science, Technology, Engineering and Management (ICSTEM'17)* held on 3rd and 4th March, 2017 at KIT- Kalaignarkarunanidhi Institute of Technology, Coimbatore, Tamilnadu, India.
- Presented a paper titled "Fusion of PAN and MS images using Optimization based Segmentation Techniques" in the *International Conference on Advanced Information and Communication Technology (ICAIC'17)* held on 24th and 25th February, 2017 at Karpagam College of Engineering, Coimbatore, Tamilnadu, India.
- Presented a paper titled "Segmentation based Satellite Image Fusion" in the *International Conference on Data Science and Engineering (ICDSE'17)* held on 20th and 21th January, 2017 at PSG College of Technology, Coimbatore, Tamilnadu, India.

KIT - Kalaignarkarunanidhi Institute of Technology

(Accredited with 'A' Grade by NAAC)
(Approved by AICTE, New Delhi & Affiliated to Anna University, Chennai)
KIT Global Institute for Advanced Studies & Research
Coimbatore-641 402, Tamilnadu, India.

ISO 9001:2008

Certificate of Appreciation

This is to certify that ~~Dr./Mr./~~Ms./~~Prof~~ S.VARSHALAKSHMI *of* KUMARAGURU COLLEGE OF TECHNOLOGY *has presented a paper titled* SATELLITE IMAGE FUSION USING CLUSTERING ALGORITHMS *in ICMR sponsored* ***IEEE International Conference on Science, Technology, Engineering and Management (ICSTEM'17)*** *held on 3rd and 4th March, 2017 at KIT - Kalaignarkarunanidhi Institute of Technology, Coimbatore, Tamilnadu, India.*

Dr. R. Sukumar	**Dr. P.Anbalagan**	**Dr. N.Mohan Das Gandhi**
Organizing Chair	*Director*	*Principal*

In Association with

IEEE MADRAS SECTION

ICAIC 17 KCE

KARPAGAM
COLLEGE OF ENGINEERING
Rediscover | Refine | Redefine
Coimbatore - 641032
Autonomous | Affiliated to Anna University, Chennai
Accredited by NAAC With 'A' Grade | Accredited by NBA (ECE, EEE, CSE and IT)

ICMR Sponsored

ICAIC-17

CERTIFICATE

Knowledge Partners

This is to certify that Dr. / Mr./ Ms.

VARSHALAKSHMI.S, KUMARAGURU COLLEGE OF TECHNOLOGY

has participated / presented a paper in the **International Conference**

on Advanced Information and Communication Technology (ICAIC-17) during 24th and 25th February 2017,

organized by the Department of Computer Science & Engineering and Information Technology

Karpagam College of Engineering, Coimbatore, Tamilnadu, India.

Paper Title FUSION OF PAN AND MS IMAGES USING OPTIMIZATION BASED SEGMENTATION TECHNIQUES

Co-ordinator | Executive Organizing Secretary | Convenor | Principal

DEPARTMENT OF COMPUTER SCIENCE & ENGINEERING

PSG COLLEGE OF TECHNOLOGY

(GOVT. AIDED AUTONOMOUS INSTITUTION, AFFILIATED TO ANNA UNIVERSITY, CHENNAI)

COIMBATORE - 641004

Certificate of Participation

This is to certify that Dr./Mr./Ms. VARSHALAKSHMI S *of* KUMARAGURU COLLEGE OF TECHNOLOGY *has presented a paper titled* SEGMENTATION BASED SATTELITE IMAGE FUSION *at the international conference on Data Science & Engineering (ICDSE '17) organised by Department of Computer Science & Engineering at PSG College of Tehcnology, Coimbatore during 20-21 January, 2017.*

P. Sampath Kumar

Mr. P. Sampath Kumar / Ms. C. Kavitha
Organising Secretaries

gsudha

Dr. G. Sudha Sadasivam
Co-Convenor

Venkatesan

Dr. R. Venkatesan
Convenor

Dr. R. Rudramoorthy
Principal